MICROSCOPIC EXPERIMENTAL STUDY ON ACOUSTIC AGGLOMERATION OF THE DROPLETS ON WALL

by

Fang-Fang LI[a], Chen HUANG[a], En XIE[a], Guang-Qiang WANG[b,c], and Jun QIU[b,c*]

[a] College of Water Resources and Civil Engineering, China Agricultural University, Beijing, China
[b] State Key Laboratory of Hydroscience and Engineering, Tsinghua University, Beijing, China
[c] State Key Laboratory of Plateau Ecology and Agriculture, Qinghai University, Xining, China

Original scientific paper
https://doi.org/10.2298/TSCI200309233L

Study on the effect of acoustic wave on droplet collision-coalescence process is interesting and helps to better understand the acoustic agglomeration mechanism. This study designs and carries out a microscopic experiment to investigate the effect of acoustic wave on wall droplet collision-coalescence process. The derived microscopic images of droplets under the action of different sound waves at different moment are processed and analyzed by binaryzation with iterative threshold, cavity filling, morphological open arithmetic processing, and identification of connected regions, etc. Using a newly defined parameter, equivalent droplet size, the growth rates of the droplets in natural state and under the action of different acoustic parameters are compared and analyzed. The results show that the effect of sound wave greatly accelerates the collision-coalescence process of the droplet, and comparing with sound pressure level, the frequency of the sound wave is a more effective parameter in promoting the collision-coalescence process of wall droplets, and the lower the acoustic wave frequency results in larger collision-coalescence rate.

Key words*: droplet collision-coalescence process, microscopic image processing, acoustic agglomeration, acoustic frequency, sound pressure level*

Introduction

A number of studies have verified the phenomena of acoustic agglomeration of different types of particles occurring in various physical processes. Xi *et al.* [1] observed regular movement of small particles (diameter < 30 μm) towards wave nodes under the action of strong standing wave acoustic field (sound pressure level, SPL > 150 dB). Hou *et al.* [2] found that the acoustic wave with low frequency and high sound intensity is more conducive to fog dissipation in the experiments of acoustic fog dissipation. Hoffmann [3] reported the acoustic wake effect observed in experiments for the first time. Hoffmann and Koopmann [4] observed the phenomena of tuning fork agglomeration under the action of two perpendicular sound velocity fields under the microscope. Hoffmann [5] demonstrated acoustic dissipation of small aerosol particles in the air by pilot scale test. Gonzalez *et al*. [6] proved for the first time the dominant role of acoustic wake effect in acoustic agglomeration by experiments.

There are many parameters influencing the agglomeration process of particles in acoustic agglomeration, such as the frequency of sound wave, SPL, sound field structure, par-

* Corresponding author, e-mail: aeroengine@tsinghua.edu.cn

ticle concentration, particle size distribution, temperature and action time, *etc*., of which, the frequency is the most discussed parameter. Based on the mechanism of co-directional motion, if the frequency is too small, all the particles in the sound field will oscillate synchronously without relative motion. While if the frequency is too large, the particles will basically be in a stable and static state, thus the collision probability of the particles is low in both cases, and the effect of acoustic agglomeration is not obvious. Based on the mechanism of hydrodynamics, the hydrodynamic force increases with the increase of the frequency of sound wave, therefore, there exists an optimal acoustic frequency to make the agglomeration effect of fine particles more obvious. Caperan *et al*. [7] found that for the particles with an average particle size of 0.8 μm, the sound wave of 21 kHz is more effective than that of 10 kHz. Gallego-Juarez *et al*. [8] and Riera-Franco *et al*. [9] derived similar conclusions in the study of acoustic agglomeration process of submicron ultrafine particle emissions from fluidized bed boilers and Diesel engines, respectively. Li *et al*. [10] theoretically studied the motion of cloud droplets due to a traveling sound wave field using the motion equation of point particles, and concluded that when SPL < 100 dB and frequency >500 Hz, the acoustic agglomeration effect is negligible. Liu *et al*. [11] found that acoustic field with low frequency is more conducive to fly ash agglomeration in coal-fired power plants than that with high frequency, and under the action of 1400 Hz acoustic wave, the agglomeration proportion of particles reaches the maximum value of 75.3%. Sun [12] added acoustic coupling jet to Liu *et al*. [11] experiment to enhance the agglomeration effect of particles, and obtained the optimum frequency of 1416 Hz. Zhou [13] established an experimental model with a spray system to study the acoustic agglomeration mechanism with different acoustic frequency, SPL, spray flow rate and surfactant type and concentration, and concluded that 1000~1800 Hz is the most suitable frequency range for the acoustic agglomeration.

Due to the complexity of the acoustic agglomeration mechanism, the optimal acoustic frequency under different experimental conditions cannot be generalized. Generally speaking, the smaller the average particle size is, the higher the optimal acoustic frequency is.

Another important parameter in acoustic agglomeration is SPL. The propagation of sound wave is accompanied by the propagation of energy. Sound intensity is defined as the energy per unit area perpendicular to the direction of sound wave propagation in a unit time, which is also called SPL when expressed by sound pressure with the unit of decibel. Sound field with higher SPL has higher energy, where the vibration amplitude and relative displacement of particles increases, thus the probability of agglomeration increases after collision, and the effect of acoustic agglomeration is better. Chen *et al.* [14] found that the SPL was proportional to the agglomeration efficiency under the same condition when studying the effect of sound field intensity on the removal efficiency of PM2.5 particles. Zhou *et al*. [15] and Komarov *et al*. [16] got the similar conclusions in the experiments on acoustic agglomeration of mixed aerosol particles composed of coal-fired fly ash and air, and Zn particles, respectively.

The influence of other experimental parameters on acoustic agglomeration is also obvious. Scott [17] considered that the efficiency of acoustic agglomeration decreased with the decrease of the concentration of particulate matter in soot. Ma *et al.* [18] found that the agglomeration efficiency of fly ash from coal-fired power plants would be significantly improved by combining sound field with wet spray. Hoffman *et al.* [19] added $CaCO_3$ particles with average size of 88 μm into fly ash to improve the agglomeration effect.

After the 1990, scholars began to use micro high speed photography to record the morphological characteristics of the growth process of particles under the action of sound wave, and quantitatively describe it by digital image processing technology. In recent years, scholars have done a lot of experiments on acoustic agglomeration, and made preliminary accomplish-

ments on both the agglomeration mechanism and numerical simulation. Wei *et al.* [20] even conducted field experiments on acoustic precipitation in Qinghai-Tibet Plateau in China. However, due to the complexity of the system of agglomeration, existing models are too rough to be used as a criterion determine the optimal model parameters compared with the actual process. On the other hand, most of the current acoustic agglomeration experiments choose coal-fired fly ash or air soot as the experimental object, and it is necessary to verify whether its effect is similar to that of droplet.

In this paper, the effect of acoustic wave on agglomeration process of droplets on the wall is studied by microscopic experiments. A micro-experiment system mainly composed of spraying device, acoustic generator, and a microscopic observation device is firstly designed and set up. The agglomeration process is recorded under sound waves with different frequency and SPL. Then all the observed microscopic images are processed and analyzed to quantify the characteristics of the droplets at different time. Finally, the quantitative relationship between the growth rate of droplets on the wall and the acoustic characteristic parameters, mainly the frequency and SPL, is obtained.

Experiment

Experiment system

There are four parts composing the experiment system:

- *Droplet generator device*: it is composed of a humidifier, a silica gel hose with an inner diameter of 19 mm and an inverted measuring cup of 1000 mL. The inverted measuring cup forms a cavity, and the liquid droplets diffuse freely into the air from the rectangular outlet at the bottom of the measuring cup after filling the cavity. The diameter of droplets coming out of the humidifier is between 7-17 μm, which can imitate the cloud droplets. In the design of the experimental device, the length of the silica gel hose connecting the humidifier and the measuring cup should be as short as possible to avoid the accumulation and growth of droplets on the inner surface of the hose and the influence of the cross-sectional area through the hose.
- *Microscopic observation device*: a digital microscope is equipped with microscopic imaging system, which can synchronously preview the physical images under the microscope through digital-analog conversion on the computer, and obtain the image and video of the agglomeration process of droplets on the slide. The magnification of the microscope is 100 times.
- *Acoustic wave generator*: a mathematical model of single frequency of sinusoidal sound wave is established, connected with an acoustic amplifier. The frequency selected in this experiment are 30 Hz, 50 Hz, 80 Hz, and 100 Hz, respectively, and the SPL is controllable.
- *Acoustic measurement device*: the sound field around the slide is dynamically monitored by a hand-held acoustic analyzer, so as to maintain a stable sound field intensity during the experiment. The selected SPL are 70 dB, 80 dB, 90 dB, and 100 dB, respectively. It needs to be illustrated that sound pressure is the change of atmospheric pressure caused by acoustic disturbance, *i.e.*, the residual pressure of atmospheric pressure, SPL is thus defined:

$$SPL = 20\log_{10}\left[\frac{P_e}{P_{ref}}\right] \tag{1}$$

where P_e is the effective sound pressure to be measured and P_{ref} – the reference of the sound pressure, usually equal to $2 \cdot 10^{-5}$ Pa.

Figure 1 shows the schematic diagram and the equipment pictures of the experimental device.

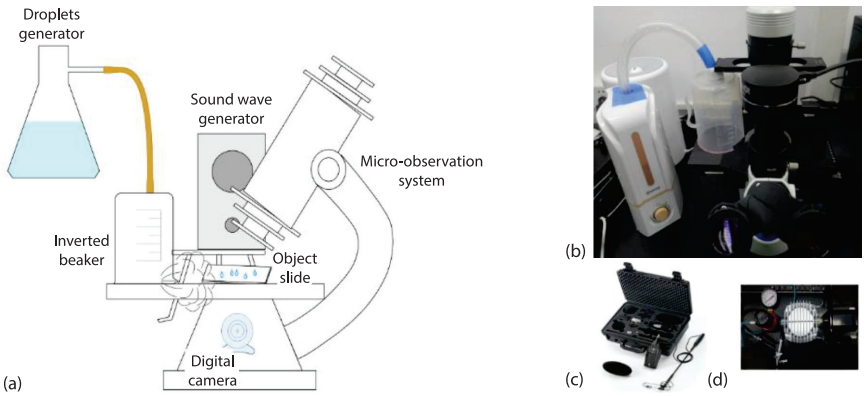

Figure 1. Experimental device; (a) schematic diagram of experimental set-up, (b) pictures of the devices, (c) hand-held acoustic measuring equipment, and (d) air pump

Experiment implementation

To avoid the influence of temperature change on droplet collision-coalescence process, the objective table of the microscope is kept under a constant temperature of 25 ±1 °C. The laboratory is airtight without ventilation avoid disturbance of air-flow on the natural dispersal of droplets above the slide and affect the collision-coalescence efficiency.

This experiment is a multi-variable design experiment. On the premise of confirming that there is no interaction among the decomposed variables, the multi-variable experiment is decomposed into a single variable experiment, in which the only variable is controlled to eliminate the interference of other factors. In this study, the frequency of sound wave is set as 30 Hz, 50 Hz, 80 Hz, and 100 Hz, respectively, and the SPL is set as 70 dB, 80 dB, 90 dB, and 100 dB, respectively. Hence, there are 16 groups of experiments. Each group of experiments is repeated five times to improve the controllability of the experimental process. The results are the average of five parallel experimental results.

Before each experiment:

– the glass slide is wiped repeatedly with alcohol cotton cloth along the same direction prevent the effect of oil stains on the surface of the glass on the morphology of droplets,
– the air is supplied into the cavity formed by the inverted measuring cup with an air pump to discharge the remaining liquid droplets from the last experiment, and
– the humidifier opening is set at the same position maintain the spray flow rate, the initial diffusion velocity of the droplets and the concentration of droplets in the cavity as stable as possible.

The whole process of droplet collision-coalescence is recorded for two minutes, and the microscopic image is obtained every 20 seconds by the microscopic imaging system.

Methodology of microscopic image processing

Overview of the methodology

As an information carrier, image accurately records the related information of the object. Digital image is obtained by digitizing analog image. It is a sampled and quantized 2-D

function, which is expressed by array or matrix. The digital matrix of a digital image $f(x, y)$ with the size of $M \times N$ is shown:

$$f(x,y)\begin{bmatrix} f(0,0) & \cdots & f(0,N-1) \\ \vdots & \ddots & \vdots \\ f(M-1,0) & \cdots & f(M-1,N-1) \end{bmatrix} \tag{2}$$

Each function in the matrix array represents a pixel, and its value represents the color and gray value of the pixel.

Image enhancement

Image enhancement is an important way to improve the visual effect of images. Due to various uncertainties, in the process of generating and transmitting the microscopic images, the image quality will be inevitably uneven, the clarity will decline, and the droplet morphology characteristics will be submerged, which makes it difficult to develop image processing algorithms to extract the statistical morphology index of the droplets. Image enhancement is used to highlight the interested parts in the image according to the specific needs, such as enhancing the high frequency component in the image to clarify the contour of the object; and enhancing the low frequency component can reduce the noise effect in the image.

Image enhancement includes spatial domain enhancement and frequency domain enhancement. Spatial domain refers to the set of pixels constituting the image. Spatial domain enhancement mainly operates on each pixel in the image, which is transformed into the gray value determined by the neighborhood pixels, mainly including gray transformation enhancement, histogram transformation enhancement, smoothing enhancement, median filtering, template filtering and high energy filtering*, etc.* Frequency domain enhancement transforms the image from the original image space into a frequency domain space in some form, so that the information can be represented as a combination of components with different frequency, mainly including low pass filtering, high pass filtering, band-stop filtering and homomorphic filtering.

Comparing the effects of different image enhancement methods on droplet images, the median filtering algorithm is adopted in this study to directly calculate the gray level of the image. The basic principle of median filtering is that the value of a point in a digital image or matrix series is replaced by the median of neighborhood points. The denoising effect of median filtering is quite obvious for droplets images, in which the gray values of the image pixel changes little.

Image segmentation

Image segmentation is to divide the image space into several specific regions according to the corresponding conditions to simplify the process of extracting interested objects and reduce the amount of data in image analysis and recognition. Threshold image segmentation is one of the most basic methods, the basic principle of which is to select gray thresholds, and then compare the gray values of each pixel in the image with the thresholds. According to the results of comparison, the pixels are divided into two or more categories, thus the image is divided into non-overlapping region sets. In this paper, an iterative threshold segmentation method is used to binarize the microscopic image of droplet agglomeration process. The procedures are:

- taking the average gray value, T_0, of the image as the initial threshold, then
- dividing the pixel points of the image into two parts by T_0, and
- calculating the average gray value of each part, the parts with the average value less than T_0 is recorded as T_A, and the parts with the average value greater than T_0 is recorded as T_B,

– calculating the average value T_1 of T_A and T_B, and
– replacing T_0 with T_1 as the new threshold for the whole image, and repeating the aforementioned procedures until T_k converges.

Figure 2 shows the pre-and post-binarization image of the droplet agglomeration process.

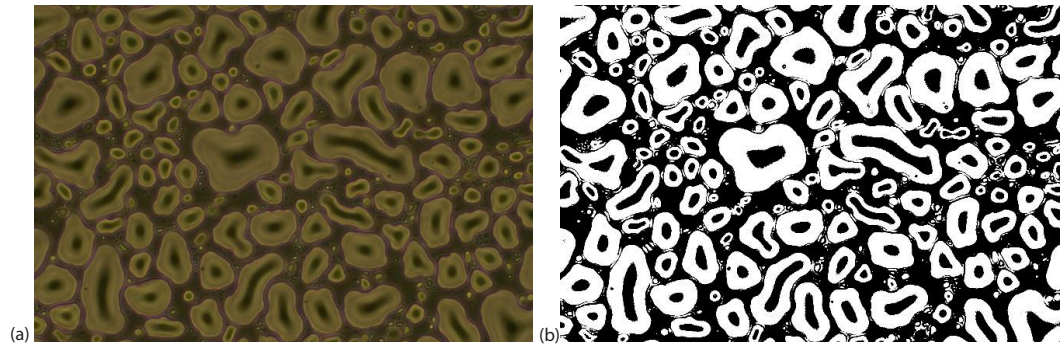

Figure 2. Comparison of the droplets microscopic images; (a) before and (b) after the iterative binarization

Image morphological processing

Image morphological processing includes four basic operations: expansion, corrosion, opening, and closing operations. Morphological processing is implemented with the help of a small shape or template (structural element). Structural element is a neighborhood specially defined. By decomposing the neighborhood, the execution speed can be improved.

Expansion refers to adding pixels to the edge of the object and merging the background points without droplet into the object, so that two droplets close to each other can be connected to form a droplet. Corrosion is to eliminate the boundary points of the object, which can remove the objects smaller than structural elements and separate two objects with fine connections. The operation of first corrosion and then expansion is called open operation, which is used to smooth the boundary contour of the object, disconnect the narrow adherent parts and eliminate the small protrusion. The operation of first expansion and then corrosion is called closed operation, which can also smooth the boundary contour of the object, but bridge the narrow discontinuity and long gullies, fill the break in the contour line and connect the adjacent objects.

As shown in fig. 2, since the gray values of the background of the original image and that of the droplet center are close, the central convex portion of the droplets is classified into the background and thus forms voids after iterative binaryzation, resulting in incomplete droplet shape. Therefore, the isolated internal pixel points, *i.e.*, the zeros surrounded by one, are filled, and the result is shown in fig. 3.

The noise of the binary image after the cavity filling is still quite obvious with rough edges, adhered droplets and narrow and slender connecting parts between droplets, which interferes the identification of the connected domain, as well as the calculation of the characteristic parameters. Therefore, the open operation is performed to smooth the edge of the droplets, and eliminate the small objects. The image after open operation is shown in fig. 4.

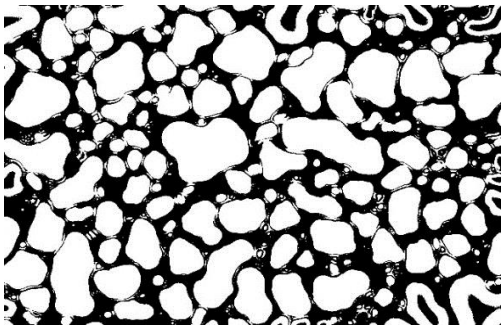

Figure 3. Image after void filling

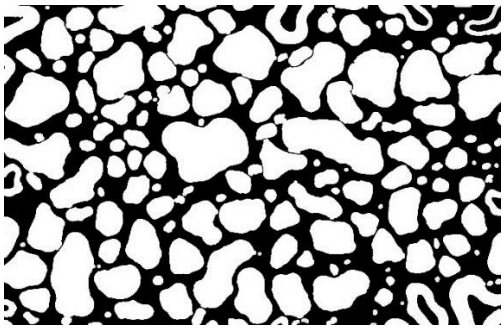

Figure 4. Image after open operation

Recognition of the connected regions

The target droplets are extracted in the form of binary images after the image segmentation and image morphological processing with the pixel values of 1. To further analyze the characteristics of the droplets, it is necessary to recognize the connected regions in the binary image.

The first step of recognizing connected regions is to assign the same number to all the pixels belonging to the same connected region and assign different numbers to different connected regions, called connected region tag. Connectivity mainly includes four connectivity and eight connectivity. In this study, eight connectivity is applied to derive more precise results, *i.e.*, starting from one pixel in the area, any other pixel in the area can be reached by continuously moving eight adjacent pixels. Taking the image in fig. 5 for instance, the original matrix is BW, and the output matrix after the operation of L = bwlabel (BW, 8) is L. As can be seen from the output matrix, the function bwlabel marks two regions in the original image, represented by 1 and 2, respectively:

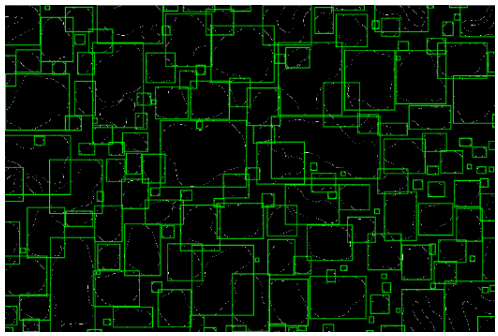

Figure 5. Recognition result of the connected region on the binary image

$$BW = \begin{bmatrix} 0 & 0 & 0 & 00 & 0 & 0 & 0 \\ 0 & 1 & 1 & 00 & 1 & 1 & 1 \\ 0 & 1 & 1 & 00 & 0 & 1 & 1 \\ 0 & 1 & 1 & 00 & 0 & 0 & 0 \\ 0 & 0 & 0 & 11 & 0 & 0 & 0 \\ 0 & 0 & 0 & 11 & 0 & 0 & 0 \\ 0 & 0 & 0 & 11 & 0 & 0 & 0 \\ 0 & 0 & 0 & 00 & 0 & 0 & 0 \end{bmatrix} \quad L = \begin{bmatrix} 0 & 0 & 0 & 00 & 0 & 0 & 0 \\ 0 & 1 & 1 & 00 & 2 & 2 & 2 \\ 0 & 1 & 1 & 00 & 0 & 2 & 2 \\ 0 & 1 & 1 & 00 & 0 & 0 & 0 \\ 0 & 0 & 0 & 11 & 0 & 0 & 0 \\ 0 & 0 & 0 & 11 & 0 & 0 & 0 \\ 0 & 0 & 0 & 11 & 0 & 0 & 0 \\ 0 & 0 & 0 & 00 & 0 & 0 & 0 \end{bmatrix} \tag{3}$$

In a binary image, area is the geometric indicator measuring the size of the connected region, which is defined as the total number of pixels in the connected region. Figure 5 shows the recognition results of the connected regions, in which the green frames represent the minimal rectangles capable of covering the connected regions, and the area of the green frames are taken as that of the connected regions.

Results

Images derived from the experiments

The images of droplet agglomeration process obtained from the designed experiment are shown in fig. 6, which shows the process under natural condition and under the action of sound waves of 70 dB/30 Hz, 70 dB/50 Hz,, 70 dB/80 Hz, and 70 dB/100 Hz, respectively.

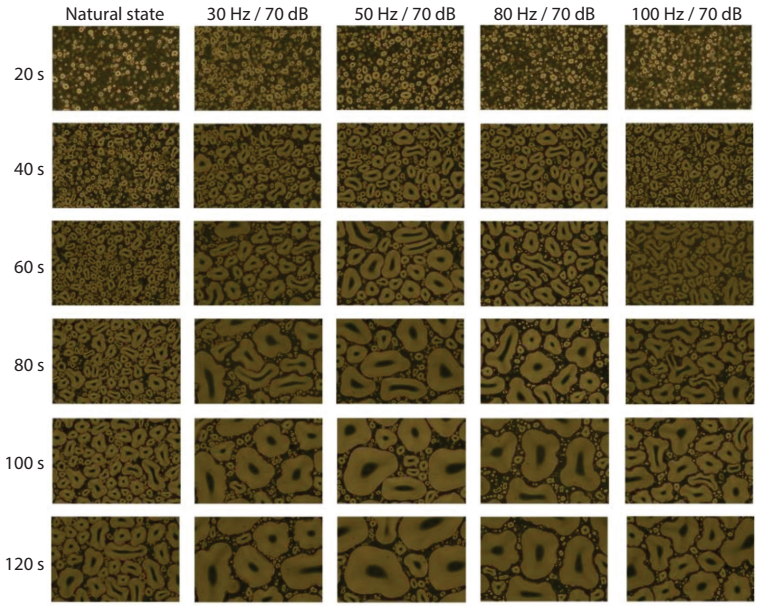

Figure 6. Droplet agglomeration process under natural condition and sound waves with different frequency and SPL at different moment

Distribution of weighted average droplet size of droplets

Based on the image processing aforementioned method, an area distribution matrix of droplets is obtained. The droplet size is represented by the equivalent diameter obtained from the area, and the weighted average droplet size at each moment is obtained:

$$D = \sum_{i=1}^{n} \frac{d_i s_i}{S} \tag{4}$$

where D [μm] is the weighted average droplet size at a certain moment, d_i [μm] – the equivalent diameter of the i^{th} droplet, s_i [μm^2] – the area of the i^{th} droplet at the moment, and S [μm^2] – the total area of all the droplets at the moment.

Table 1 shows the particle size changes during the droplet collision-coalescence process on the wall without sound waves and under the action of sound waves with different frequencies and SPL.

Growth rate of droplets

The droplet collision-coalescence process curve within 2 minutes is derived from the weighted average particle size at different moment in tab. 1, and a linear fitting is performed, as shown in fig. 7. The degrees of fitting are all above 0.97. The slope of the linear equation indicates

Table 1. Particle size changes during the droplet collision-coalescence process on the wall under the action of different sound waves

Frequency [Hz]					SPL [dB]	Weighted average droplet size at a different moments [μm]						Maximal size [μm]
						20 s	40 s	60 s	80 s	100 s	120 s	
Without sound wave						15	29	48	63	91	112	158
30	100	26	63	113	148	183	224			329		
	90	26	59	104	150	175	225			326		
	80	23	56	90	121	145	174			244		
	70	26	62	100	136	180	226			333		
50	100	31	58	91	133	174	208			324		
	90	34	66	105	135	183	222			300		
	80	30	62	94	139	179	205			309		
	70	33	67	115	142	184	224			329		
80	100	25	50	83	121	149	187			259		
	90	27	52	81	118	156	185			255		
	80	27	54	80	115	151	181			245		
	70	30	54	99	136	174	204			260		
100	100	23	41	57	83	109	145			203		
	90	22	40	62	88	124	163			231		
	80	21	29	66	97	121	158			208		
	70	23	41	78	114	136	167			220		

the collision-coalescence rate of the droplets on the wall under acoustic waves with different frequencies and SPL. Figure 7 shows the natural collision-coalescence process curve of droplets without sound waves, as well as those under sound wave action with different frequency and SPL.

The experimental data and fitting curves show that the effect of sound waves greatly accelerates the collision-coalescence process of wall droplets. The weighted average particle diameter, D, of the droplets at a certain moment has a linear relationship with time, t, *i.e.*, $D = kt + b$, where k is the average growth coefficient of the droplets. During the collision-coalescence process, the average growth coefficient of the droplets reflects the droplet capability of absorbing the water vapor in the air and seizing the surrounding droplets. Table 2 shows the average growth coefficients of droplets under natural conditions and different sound waves.

Table 2. Average growth coefficients of droplets under natural conditions and different sound waves

SPL [dB] / Frequency [Hz]	30	50	80	100
00	1.9786	1.8209	1.6344	1.2025
90	1.9764	1.8876	1.6271	1.3981
80	1.5108	1.8157	1.5657	1.3739
70	1.9833	1.9026	1.8114	1.4863

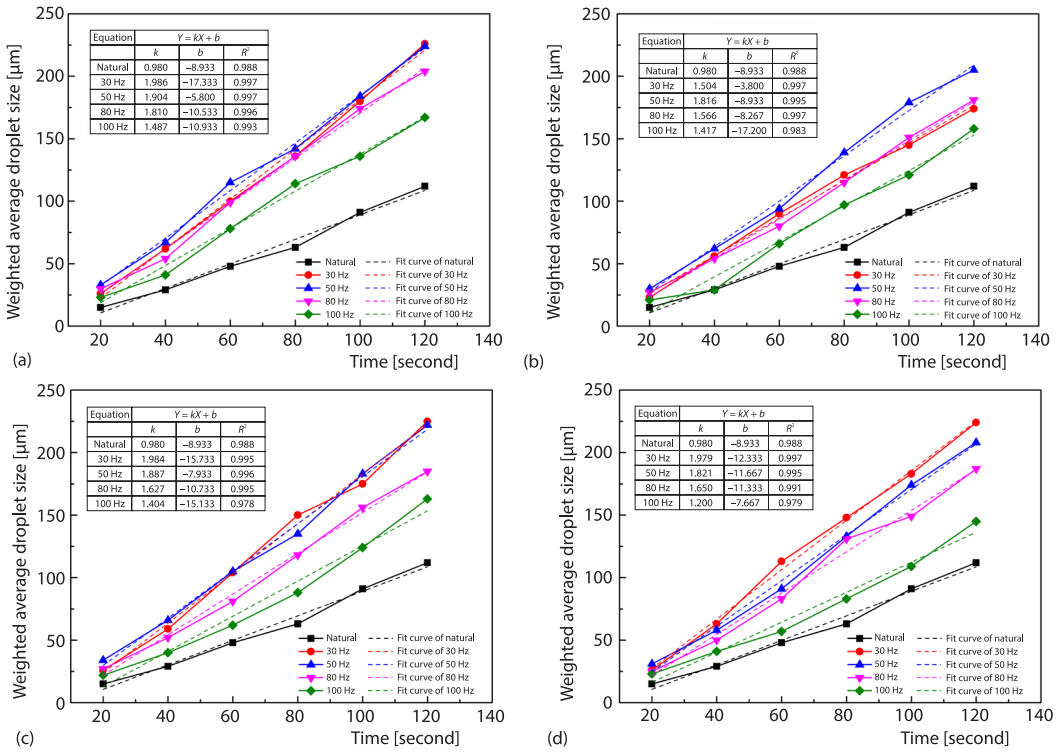

Figure 7. Collision-coalescence process curves of droplets under the sound wave of (a) 70 dB, (b) 80 dB, (c) 90 dB, and (d) 100 dB with different frequency, as well as the linear fitting curves and the fitting equations

Discussion

It can be seen from the results that under the same SPL, the droplets coagulate with a larger growth rate under a lower acoustic frequency, *i.e.*, the growth rate of the droplets is increasing corresponding to the sound waves of 100 Hz, 80 Hz, 50 Hz, and 30 Hz, respectively.

Under the action of sound wave of 100 Hz, the maximum average growth coefficient of droplets k_{max} is 1.4863, while under the action of sound waves of 80 Hz, k_{max} is 1.8114, which is 22% higher than that at 100 Hz. The k_{max} under sound wave of 50 Hz is 1.9026, 5% higher than that at 80 Hz. While k_{max} under sound wave of 30 Hz is 1.9833, which is 4% higher than that at 50 Hz. It can be inferred that as the frequency of the sound wave decreases, the increase rate of droplet growth rate k slows down.

Under the same frequency, there is no obvious change of the droplet collision-coalescence rates for sound waved with different SPL. The all sound waves of different frequency have the greatest effect on the collision-coalescence process of wall droplets at the SPL of 70 dB.

Under the action of 30 Hz and 70 dB sound wave, the average growth coefficient of the wall droplets reaches the maximal value of 1.9833, which is about 2.02 times of that under the natural condition, and the maximum equivalent diameter of the droplets is 333 μm. Under the action of sound wave of at 100 Hz and 100 dB, k is minimal with the value of 1.2025, which is about 1.23 times of that in the natural state, and the maximum equivalent diameter of the droplets is 203 μm.

In the experiments, under the natural condition, there are droplets freely diffusing in the air above the upper surface of the slide with a certain initial velocity, and collide with the slide surface, as shown in fig. 8. A large number of randomly and uniformly distributed initial droplets are formed instantaneously. The size of the wall droplet becomes larger and larger due to the collisions merge between droplets, resulting from continuous action of the droplet generator and continuous collision-coalescence process of the water vapor around the initial droplet.

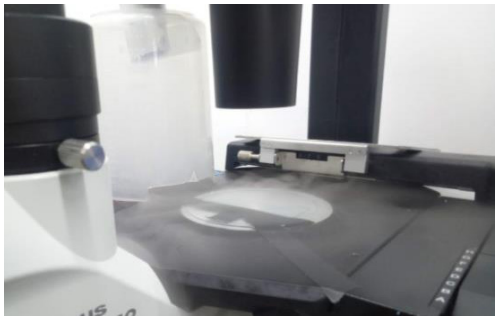

Figure 8. Droplets diffusion above the glass slide

Under the action of sound waves, the sound field of lower frequency is more conducive to the growth of wall droplets. When a low frequency sound wave acts on a droplet, the droplet vibrates. Due to the difference of droplet size and inertia, and the vibration amplitude increases as the particle size decreases. Based on the mechanism of the same-direction motion, relative movements occur between droplets of different sizes. At the same time, the action of sound waves causes disturbance of air around the droplets, resulting in an increased probability of colliding between droplets and an increase in droplet collision-coalescence rate.

Since the research background of this experiment is to simulate cloud droplets, the tiny droplets formed in the droplet generator are transparent, and the droplets are convex when condensed on the surface of the slide, the highest part of the protrusion forms a plane, the RGB of which is close to that of the background in the digital images. It brings difficulties to the post-image processing. How to dye the droplets without affecting the bulk density and collision-coalescence characteristics of the droplets is a problem to be solved.

During the experiment, due to the continuous action of the droplet generator and the heat transfer effect of the droplet collision-coalescence process, slight temperature changes occur on the surface of the slide, which may induce some thermodynamics process related to droplet growth, and thus affect the rate of droplet collision-coalescence process.

Conclusion

In this paper, a microscopic experiment is designed to investigate the effect of acoustic wave on wall droplet collision-coalescence process. The microscopic images are processed to quantitively analyze the collision-coalescence characteristics of droplets under the sound wave with different frequency and SPL. The image process mainly includes iterative binarization, hole filling, morphological open operation, connected region recognition, and droplet feature parameter extraction.

The particle size distribution of the droplet collision-coalescence process is calculated from the area distribution matrix, and the weighted average particle size of the droplet is linearly fitted with the growth time for different acoustic frequencies and different SPL. The defined growth coefficient reflecting the droplet collision-coalescence rate indicates that comparing with SPL, the frequency of the sound wave is a more effective parameter in the promotion of the collision-coalescence process of wall droplets, and the lower the acoustic wave frequency results in larger collision-coalescence rate.

Acknowledgment

This research was founded by National Natural Science Foundation of China (Grant No. 91847302, 51879137, 51979276).

References

[1] Xi, B. S., *et al*., Experiments on Tiny Particles Effected by in-Tense Standing Wave Field, *Experiments and Measurements in Fluid Mechanics*, *142* (2000), 2, pp. 49-53
[2] Hou, S. Q., *et al*., Experiments on Acoustic Dissipation of Water fog at Low Frequency, *Experiments and Measurements in Fluid Mechanics*, *16* (2002), 4, pp. 52-56
[3] Hoffmann, T. L., An Extended Kernel for Acoustic Agglomeration Simulation Based on the Acoustic Wake Effect, *Jounal Aerosol Sci*., *28* (1997), 6, pp. 919-936
[4] Hoffmann, T. L., Koopmann, G. H., Visualization of Acoustic Particle in-Teraction and Agglomeration: Theory and Experiments, *Journal Acoust. Soc. Am*, *99* (1996), 4, pp. 2130-2141
[5] Hoffmann, T. L., Environmental Implications of Acoustic Aerosol Agglomeration, *Ultrasonics*, *38* (2000), 1-8, pp. 353-357
[6] Gonzalez, I., *et al*., The Influence of Entrainment on Acoustically Induced Interactions between Aerosol Particles – An Experimental Study, *Journal Aerosol Sci.*, *34* (2003), 12, pp. 1611-1631
[7] Caperan, P., *et al*., Acoustic Agglomeration of a Glycol fog Aerosol – Influence of Particle Concentration and Intensity of the Sound Field at 2 Frequencies, *Journal Aerosol Sci*., *26* (1995), 4, pp. 595-612
[8] Gallego-Juarez, *et al*., Application of Acoustic Agglomeration Reduce Fine Particle Emissions from Coal Combustion Plants, *Environ Sci. Technol*., *33* (1999), 21, pp. 3843-3849
[9] Riera-Franco de Sarabia, E., *et al.*, Acoustic Agglomeration of Submicron Particles in Diesel Exhausts: First Results of the Influence of Humidity at Two Acoustic Frequencies, *Journal Aerosol Sci*., *31* (2000), Sept., pp. 827-827
[10] Li, F.-F., *et al*., Mechanism of Cloud Droplet Motion under Sound Wave Actions, *Journal Atmos Oceanic Technol*., *37* (2020), 9, pp. 1539-1550
[11] Liu, J. Z., *et al*., Frequency Comparative Study of Coal-Fired fly Ash Acoustic Agglomeration, *Journal Environ Sci-China*, *23* (2011), 11, pp. 1845-1851
[12] Sun, D. S., Investigation into Agglomeration Processs of Inhalable Particle in Coupling Acoustic Wave and JET, Ph. D. thesis, Qingdao University of Science and Technology, Qingdao, China, 2009
[13] Zhou, D., Experimental Researches and Simulation on Acoustic Agglomeration of Various Particle Sources, Ph. D. thesis, Zhejiang University, Hangzhou, China, 2016
[14] Chen, H. T., *et al*., Experimental Study on Acoustic Agglomeration of Ultrafine Fly Ash Particles, *Proceedings of the CSEE*, *27* (2007), 35, pp. 28-32
[15] Zhou, D., *et al*., Experimental Study on Improving the Efficiency of Dust Removers by Using Acoustic Agglomeration as Pretreatment, *Powder Technol.*, *289* (2016), Feb., pp. 52-59
[16] Komarov, S. V., *et al*., Acoustically Controlled Behavior of Dust Particles in High Temperature Gas Atmosphere, *ISIJ International*, *44* (2004), 2, pp. 275-284
[17] Scott, D. S. A New Approach to the Acoustic Conditioning of Industrial Aerosol Emissions, *Journal Sound Vib*, *43* (1975), 4, pp. 607-619
[18] Ma, D. G., *et al*., Pretreatment Based on Combined Effect of Acoustic Agglomeration and Atomization and Its Application in Air Filtration, *Chinese Journal of Environmental Engineering*, 9 (2015), 5, pp. 2353-2358
[19] Hoffmann, T. L., *et al*., Experimental and Numerical-Analysis of Bimodal Acoustic Agglomeration, *Journal Vib Acoust*, *115* (1993), 3, pp. 232-240
[20] Wei, J. H., *et al*.. Cloud and Precipitation Interference by Strong Low-Frequency Sound Wave, *Sci. China Technol. Sc*, *64* (2021), Apr., pp. 261-272

Paper submitted: March 9, 2020
Paper revised: August 15, 2020
Paper accepted: August 16, 2020